Laboratory photochemical processing of aqueous aerosols: formation and degradation of dicarboxylic acids, oxocarboxylic acids and α-dicarbonyls

C. M. Pavuluri[1], K. Kawamura[1], N. Mihalopoulos[1, 2, 3] and T. Swaminathan[4]

[1]Institute of Low Temperature Science, Hokkaido University, Sapporo 060-0819, Japan

[2]Environmental Chemical Processes Laboratory, Department of Chemistry, University of Crete, P.O. Box 2208, 71003 Voutes, Heraklion, Greece

[3]Institute for Environmental Research and Sustainable Development, National Observatory of Athens, GR-15236 Palea Penteli, Greece

[4]Department of Chemical Engineering, Indian Institute of Technology Madras, Chennai 600036, India

Correspondence to: K. Kawamura (kawamura@lowtem.hokudai.ac.jp)

Abstract. To better understand the photochemical processing of dicarboxylic acids and related polar compounds, we conducted batch UV irradiation experiments on two types of aerosol samples collected from India, which represent anthropogenic (AA) and biogenic aerosols (BA), for time periods of 0.5 h to 120 h. The irradiated samples were analyzed for molecular compositions of diacids, oxoacids and α-dicarbonyls. The results show that photochemical degradation of oxalic (C_2) and malonic (C_3) and other C_8-C_{12} diacids overwhelmed their production in aqueous aerosols whereas succinic acid (C_4) and C_5-C_7 diacids showed a significant increase (ca. 10 times) during the course of irradiation experiments. The photochemical formation of oxoacids and α-dicarbonyls overwhelmed their degradation during the early stages of experiment, except for ω-oxooctanoic acid (ωC_8) that showed a similar pattern to that of C_4. We also found a gradual decrease in the relative abundance of C_2 to total diacids and an increase in the relative abundance of C_4 during prolonged experiment. Based on the changes in concentrations and mass ratios of selected species with the irradiation time, we hypothesize that iron-catalyzed photolysis of C_2 and C_3 diacids dominates their concentrations in Fe-rich atmospheric waters, whereas photochemical formation of C_4 diacid (via ωC_8) is enhanced with photochemical processing of aqueous aerosols in the atmosphere. This study demonstrates that the ambient aerosols contain abundant precursors that produce diacids, oxoacids and α-dicarbonyls, although some species such as oxalic acid decompose extensively during an early stage of photochemical processing.

1 Introduction

Dicarboxylic acids and related polar compounds constitute a significant fraction of water-soluble organic aerosols in the atmosphere (Kawamura and Sakaguchi, 1999; Pavuluri et al., 2010; Saxena and Hildemann, 1996). They have a potential contribution to the formation of cloud condensation nuclei (CCN) due to their water-soluble and hygroscopic properties (Giebl et al., 2002; Saxena and Hildemann, 1996). Thus diacids and related compounds have an impact on the indirect radiative forcing and hydrological cycle (Albrecht, 1989; Twomey, 1977). They also involve in a series of reactions occurring in gas phase, aerosols and atmospheric waters (Chebbi and Carlier, 1996; Wang et al., 2010b). Although diacids, oxoacids and α-dicarbonyls can be directly emitted into the atmosphere from incomplete combustion of fossil fuels (Kawamura and Kaplan, 1987) and biomass burning (Narukawa et al., 1999), they are mainly formed by secondary processes of volatile organic compounds of anthropogenic and biogenic origin (Kanakidou et al., 2005; Kawamura et al., 1996a; Kawamura and Sakaguchi, 1999). They are further subjected to photochemical oxidation during long-range transport; e.g., carbonyls to carboxylic acids (Tilgner and Herrmann, 2010) and breakdown of higher to lower diacids (Kawamura and Sakaguchi, 1999; Matsunaga et al., 1999; Wang et al., 2010a).

Molecular distributions of diacids in atmospheric aerosols have generally been reported with a predominance of oxalic (C_2) acid followed by malonic (C_3) or succinic (C_4) acid in different environments (Kawamura and Kaplan, 1987; Kawamura and Ikushima, 1993; Kawamura and Sakaguchi, 1999; Narukawa et al., 1999; Pavuluri et al., 2010). The predominance of C_2 in different environments is likely explained because it is an ultimate end product in the chain reactions of diacids and various precursors including aromatic hydrocarbons, isoprene, alkenes and α-dicarbonyls (Carlton et al., 2007; Charbouillot et al., 2012; Ervens et al., 2004b; Kawamura et al., 1996a; Lim et al., 2005; Warneck, 2003). In

59 contrast, C_4 was reported to be more abundant than C_2 in some aerosol samples collected
60 from Antarctica (Kawamura et al., 1996b), the Arctic (Kawamura et al., 2010) and over the
61 Arctic Ocean (Kawamura et al., 2012) as well as in ice core samples from Greenland
62 (Kawamura et al., 2001). In addition, a significant reduction in C_2 diacid concentration and an
63 inverse relationship between C_2 and Fe has been reported in stratocumulus clouds over the
64 northeastern Pacific Ocean (Sorooshian et al., 2013). The predominance of C_4 over C_2 in ice
65 core samples and atmospheric aerosols from polar regions, particularly in the Arctic marine
66 aerosol samples collected under overcast conditions with fog or brume event (Kawamura et
67 al., 2012) and the reduction of C_2 in cloud water, suggest that photochemical formation of C_4
68 and/or degradation of C_2 (Pavuluri and Kawamura, 2012) should be enhanced in atmospheric
69 waters.

70 However, the photochemical formation and degradation of diacids and related
71 compounds are not fully understood, particularly in aqueous phase because the composition
72 of aqueous solutions used in laboratory experiments do not reflect the complex mixture of
73 organic and inorganic aerosol constituents in the atmosphere and the experimental conditions
74 are not necessarily atmospherically relevant (Ervens et al., 2011). Hence, it is required to
75 investigate the fate of diacids and related polar compounds with photochemical processing in
76 atmospheric waters. In this study, we conducted a laboratory experiment using two types of
77 ambient aerosol samples collected from Chennai, India, which represent anthropogenic (AA)
78 and biogenic aerosols (BA). The samples were exposed to UV irradiation in the presence of
79 moisture for different time ranging from 0.5 h to 120 h and then analyzed for diacids,
80 oxoacids and α-dicarbonyls. Here, we report their molecular compositions and discuss the
81 photochemical formation and/or degradation of diacids as a function of the irradiation time.
82 Based on the results obtained, we propose possible photochemical formation and degradation
83 pathways of diacids and related compounds with atmospheric implications.

2 Materials and Methods

2.1 Atmospheric aerosol samples

In this study, we used two types of atmospheric aerosol (PM_{10}) samples that were collected in winter on January 28 (IND104) and in summer on May 25 (IND178), 2007 during daytime (ca. 06:00-18:00 h local time) from Chennai (13.03º N; 80.17º E), India using a high volume air sampler and pre-combusted (450 ºC, 4 h) quartz fiber filters. Sampling was conducted on the rooftop of the Mechanical Sciences building (~18 m a.g.l. (above the ground level)) at the Indian Institute of Technology Madras (IITM) campus. The details of sampling site and meteorology are described elsewhere (Pavuluri et al., 2010). The sample filter was placed in a preheated glass jar with a Teflon-lined screw cap and stored in darkness at -20°C prior to the experiment. Figure 1 presents ten-day backward air mass trajectories arriving in Chennai at 500 m AGL for every 6 h during the sampling periods of IND104 and IND178. Table 1 shows concentrations of elemental carbon (EC), organic carbon (OC), levoglucosan and sums of hopanes (specific biomarkers of petroleum and coal) and lipid class compounds: fatty acids and fatty alcohols, in IND104 and IND178 (Fu et al., 2010; Pavuluri et al., 2011).

The air mass trajectories showed that the air masses for the IND104 sample originated from the north Indian subcontinent passing over the Bay of Bengal (Fig. 1). In North India, anthropogenic emissions are mainly derived from fossil fuel combustion and forest fires (Lelieveld et al., 2001; Reddy and Venkataraman, 2002a). This sample is enriched with EC (Table 1). The anthropogenic signature of IND104 is further supported by high abundances of hopanes. In contrast, the air masses for the IND178 sample originated from the Arabian Sea passing over the south Indian subcontinent (Fig. 1), where the emissions from marine biota, combustion of biofuels (e.g., cow-dung) (Reddy and Venkataraman, 2002b) and livestock (Garg et al., 2001) are important. In addition, emission of volatile organic compounds (VOCs)

from tropical plant species in India is enhanced in summer (Padhy and Varshney, 2005). This sample is enriched with OC but EC is less abundant (Table 1). The biogenic signature of IND178 is supported by high abundances of fatty acids and fatty alcohols (Table 1). Hence, we consider that IND104 represents anthropogenic aerosols (AA) whereas IND178 represents biogenic aerosols (BA).

2.2 Determination of trace elements, metals and water-soluble iron species

Trace elements and metals were determined using an inductively coupled plasma mass spectrometry (ICP-MS, Thermo Electron X Series) after the acid microwave digestion of samples (a filter disc of 1.8 cm in diameter) as reported by Theodosi et al. (2010b). Recoveries obtained with the use of certified reference materials ranged from 90.0 to 104.1%. Water-soluble iron (Fe_{WS}: sum of Fe^{2+} and Fe^{3+} species) was determined spectrometrically using the Ferrozine colorimetric method developed by Stookey (1970) as reported by Theodosi et al. (2010a). Fe^{2+} was measured using the same procedure without adding the reducing agent (hydroxylamine hydrochloride), and then Fe^{3+} was estimated indirectly as the difference between Fe_{WS} and Fe^{2+}. The recovery was ~98.3% for both Fe_{WS} and Fe^{2+}.

2.3 Irradiation experiment of aerosol samples

Batch UV irradiation experiments using two aerosol samples (AA and BA) were conducted separately for 0.5, 1.5, 3.0, 6.0, 12, 18, 24, 36, 48, 72, 96 and 120 h, because both primary and secondary chemical species that are associated with aerosols can be subjected for significant photochemical processing through out their stay (i.e., up to 12 days) in the atmosphere (Warneck, 2003). In each experiment, ~12 cm^2 (ca. 3 × 4 cm) of sample filter was cut into 3~4 pieces and placed vertically in a cleaned quartz reaction vessel (cylinder, 100 ml) with the sample surface facing to UV light as depicted in Fig. 2. The sample was

fully wetted by injecting ~0.4 ml of ultra pure organic free Milli Q water and sealed with Teflon-lined screw cap under the ambient pressure. Further, the available excess Milli Q water (Fig. 2) may promote humid (RH = 100%) environment in the reaction vessel by equilibrium between water vapor and Milli Q water. The aqueous ambient aerosol sample was then irradiated with a low-pressure mercury lamp (Ushio, UL0-6DQ) that emits a UV, whose spectra are characterized by main peak at 254 nm and minor peak at 185 nm as well as broad peak at >254 nm. The experimental setup (Fig. 2) was covered with a cartoon box containing a hole on each side for the passage of ambient air, and placed in a draft chamber. The temperature around the experimental system (i.e. inside cartoon box) was equivalent to room temperature (25±1°C).

The main objective of UV irradiation with a wavelength primarily at 254 nm, rather than a solar spectrum, was to produce significant amount of hydroxyl radicals ($HO^{\bullet}$) from various sources described below that should be sufficient enough to act as the main oxidant in our experimental system. Although we do not preclude a minor photolysis of some organic compounds present in the aerosol samples by irradiation at ≤254 nm, it is well established that low molecular weight diacids, oxoacids and α-dicarbonyls including pyruvic acid and methylglyoxal have negligible absorbance at 254 nm and exhibit minimal photolysis, particularly when $HO^{\bullet}$ reactions of organics are significant (Carlton et al., 2006; Tan et al., 2012; Yang et al., 2008a). Because sulfate is abundant in non-irradiated AA and BA (Pavuluri et al., 2011), the production of organosulfates should be significant upon irradiation (Noziere et al., 2010) in both the samples. However, the sulfate contents may not have significant impact on the production rate of diacids and related compounds (Tan et al., 2009). Further, the radiation of 185 nm is mostly absorbed by water to subsequently produce $HO^{\bullet}$ and thus minimize the photolysis of organics during the experiment (Yang et al., 2008a). On the contrary, iron-dicarboxylate complexes (e.g., oxalate and malonate) can photolyze by

159 absorbing both UV-C (254 nm) and UV-A light and their photolysis rate depends on the
160 concentration of Fe in the given sample rather than the UV light wavelength (Pavuluri and
161 Kawamura, 2012; Wang et al., 2010b; Zuo and Hoigne, 1994). In addition, radiation at 254
162 nm has been reported to impose only a marginal photolysis of most of the inorganic species,
163 except for nitrate, which is one of the $HO^{\bullet}$ sources (Yang et al., 2008a).

164 The irradiation of wetted aerosol sample at 254 nm induces the formation of O_3 from
165 the dissolved O_2 followed by generation of H_2O_2, and photolysis of H_2O, NO_3^-, NO_2^-, H_2O_2,
166 $Fe(OH)^{2+}$ and certain organic compounds, and Fenton's reaction of photochemically formed
167 Fe^{2+} and H_2O_2 to produce $HO^{\bullet}$ in aqueous phase (Arakaki and Faust, 1998; Carlton et al.,
168 2006; Yang et al., 2008a). In fact, high amount of Fe, including water-soluble Fe^{2+} and Fe^{3+}
169 species, is available in both AA and BA samples (Table 1), which could promote the
170 Fenton's reaction upon UV irradiation. In addition, O_3, H_2O_2, $HOO^{\bullet}$ and NO_2 formed in
171 aqueous phase reactions may be partitioned into gas phase and generate the gaseous $HO^{\bullet}$ that
172 should be re-partitioned into aqueous phase (Arakaki and Faust, 1998). These sources of $HO^{\bullet}$
173 are similar to those of atmospheric waters: (i) gas/drop partitioning of $HO^{\bullet}$ and (ii) gas/drop
174 partitioning of O_3 followed by reaction with peroxy radical ($HOO^{\bullet}$), (iii) photolysis of H_2O,
175 NO_3^-, NO_2^-, H_2O_2, $Fe(OH)^{2+}$ and certain organic compounds, and (iv) Fenton's reaction of
176 Fe^{2+} and H_2O_2 (Arakaki and Faust, 1998).

177 Unfortunately, we could not approximate the actual concentrations of $HO^{\bullet}$ in our
178 experiments because we did not add any chemical (e.g., a standard compound whose kinetics
179 are known) in order to keep our experimental system as realistic as possible. Furthermore, the
180 formation of O_3 from the initially available O_2 (~0.94 mM) in the reaction vessel may not
181 cause the deficit of the O_2 that could potentially induce the polymerization of organics during
182 the irradiation on aerosols for several hours, because the additional O_2 could be produced

183 from the gaseous $HOO^{\bullet}$ formed by photolysis of organics and Fenton's reaction (Arakaki and
184 Faust, 1998) during the experiment.
185
186 **2.4 Measurements of diacids, oxoacids and α-dicarbonyls**
187 Immediately after the irradiation, samples were analyzed for diacids, oxoacids and
188 α-dicarbonyls using a method reported elsewhere (Kawamura, 1993; Kawamura and
189 Ikushima, 1993). Briefly, the irradiated sample filter was extracted with Milli-Q water (10
190 mL x 3) under ultra sonication for 10 min and the extracts were concentrated to near dryness
191 using a rotary evaporator under vacuum. The extracts were then derivatized with 14%
192 BF_3/n-butanol at 100°C to butyl esters and/or butoxy acetals. Both the esters and acetals were
193 extracted with *n*-hexane and then determined using a capillary GC (HP 6890) and GC-MS
194 (Thermo Trace MS). Recoveries of authentic standards spiked to a pre-combusted quartz
195 fiber filter were 73% for oxalic (C_2) acid and more than 84% for malonic (C_3), succinic (C_4)
196 and adipic (C_6) acids (Pavuluri et al., 2010). The analytical errors in duplicate analysis of the
197 aerosol filter sample are within 9% for major species. Gas chromatogram of the field and
198 laboratory blanks showed small peaks for C_2, phthalic (Ph) and glyoxylic acids.
199 Concentrations of all the species reported here are corrected for the non-irradiated field
200 blanks (Pavuluri et al., 2010).
201
202 **2.5 Quality control**
203 To examine the possible experimental errors, including the distribution of organic/inorganic
204 constituents over the filter sample, we conducted replicate experiments (n = 3) for 18 h
205 irradiation of AA sample by using the sample cut taken from different parts of the filter
206 sample for each experiment because a deviation in the results of the irradiation experiment
207 should become large if the impact of potential variance in chemical composition of aerosol at

208 different parts of the single filter, size of the filter sample used (i.e., amount of aerosols) and
209 the amount of Milli Q water added is significant. The experimental errors, including the
210 analytical errors, were found to be within 11% for major species, except for C_3 diacid (19%).
211 These results suggest that organic and inorganic constituents are well distributed over the
212 filter sample and took up water evenly distributed upon wetting. In addition, two irradiation
213 experiments were conducted to check the procedural blank by using a clean quartz filter for
214 1.5 h and 6.0 h. No peaks were detected, except for a small peak for C_2 and Ph. These results
215 indicate that the occurrence of bias during the experiment is insignificant.
216

217 **3 Results and discussion**

218 **3.1 Concentrations of trace elements, metals and water-soluble iron species**

219 Concentrations of trace elements, metals and water-soluble Fe species (Fe^{2+} and Fe^{3+})
220 determined in non-irradiated AA and BA samples are presented in Table 1. The trace
221 elements and metals in AA sample, which mainly originate from soil dust (e.g., P, Al, Ca and
222 Fe), non-ferrous metallurgical industrial activities (Cd, Cu and Zn) and fossil fuel combustion
223 (Cr, Pb and V) (Mahowald et al., 2008; Pacyna and Pacyna, 2001), are significantly more
224 abundant than in BA (by up to several times higher), except for S, Ni and Sb (Table 1). The
225 high abundances of trace metals in AA further suggest that the AA sample should contain
226 high abundances of anthropogenic organic matter. The high abundances of S, Ni and Sb in
227 BA than in AA may be due to high emissions of the S from intensive consumption of biofuels,
228 particularly cow-dung that contains higher S content (Reddy and Venkataraman, 2002b),
229 while Ni and Sb are from some specific industrial activities in southern India. Although
230 water-soluble Fe^{2+} and Fe^{3+} species are abundant in both AA and BA, their concentrations in
231 BA are 30-50% higher than in AA (Table 1). Further the fraction of water-soluble Fe (Fe_{WS}:

sum of Fe^{2+} and Fe^{3+}) in total particulate Fe (Fe_{Tot}) is 2.77% in AA whereas it is 14.6% in BA.

3.2 Molecular compositions of diacids, oxoacids and α-dicarbonyls

A homologous series of normal (C_2-C_{12}) and branched chain (iso C_4-C_6) saturated α,ω-diacids were detected in both non-irradiated and irradiated AA and BA samples as well as aliphatic unsaturated diacids such as maleic (M), fumaric (F), and methylmaleic (mM) acids and aromatic diacids such as phthalic (Ph), isophthalic (*i*-Ph), and terephthalic (*t*-Ph) acids. Diacids with an additional functional group, i.e., malic (hydroxysuccinic, hC_4), ketomalonic (kC_3), and 4-ketopimelic (kC_7) acids, were detected, together with ω-oxoacids (ωC_2-ωC_9), pyruvic acid (Pyr), and α-dicarbonyls, i.e., glyoxal (Gly) and methylglyoxal (MeGly). ωC_6 will not be reported here due to the overlapping peak on GC chromatogram.

Oxalic (C_2) acid was found as the most abundant diacid in non-irradiated samples (accounting for 54% of total diacids in AA and 53% in BA), followed by Ph (10%), C_4 (9%), C_3 (8%) and C_9 (4%) in AA and by malonic (C_3) (9%), C_4 (6%) and *t*-Ph (6%) acids in BA. Branched chain diacids were significantly lower than the corresponding normal structures in both samples. Glyoxylic (ωC_2) acid is the most abundant oxoacid, comprising 64% and 57% of total oxoacids in AA and BA, respectively, followed by Pyr (13%) and 4-oxobutanoic (ωC_4) acid (10%) in AA and ωC_4 (18%) and Pyr (13%) in BA. MeGly is more abundant than Gly in AA whereas their abundances are equivalent in BA.

3.3 Changes in concentrations of diacids and related compounds as a function of UV irradiation time

Changes in concentrations of individual and total diacids as a function of UV irradiation time in AA and BA are depicted in Fig. 3, while those of oxoacids and α-dicarbonyls as well as

257 total oxoacids and α-dicarbonyls in Fig. 4. Concentrations of C_2 diacid were sharply
258 decreased by a factor of 3-9 (from 553 ng m^{-3} to 61.7 ng m^{-3} in AA and from 339 to 118 ng
259 m^{-3} in BA) within 6 h and 12 h of UV irradiation, respectively (Fig. 3a). Then, the
260 concentrations started to increase to maximize at 24 h (292 ng m^{-3}) in AA and 18 h (306 ng
261 m^{-3}) in BA on further irradiation. They gradually decreased toward the end (120 h) of the
262 experiment (Fig. 3a). Interestingly, C_3 diacid showed a temporal variation similar to C_2 in
263 both AA and BA, except for few points (Fig. 3b). Relative abundances of C_2 in total diacids
264 gradually decreased from non-irradiated samples (54% in AA and 53% in BA) toward the
265 end (120 h) of the experiment (3.2% in AA and 9.2% in BA, Fig. 5).

266 Concentrations of ωC_2, an immediate precursor of C_2 (Kawamura et al., 1996a; Lim et
267 al., 2005; Warneck, 2003), increased with irradiation time up to 18 h in both AA and BA,
268 except for two cases (3 and 6 h) of AA, and then gradually decreased until the end (120 h) of
269 the experiment, except for one case (36 h) in AA (Fig. 4a). Pyr, Gly and MeGly, which are
270 the precursors of ωC_2 acid, are all produced by the oxidation of VOCs of anthropogenic and
271 biogenic origin (Carlton et al., 2006; Ervens et al., 2004b; Lim et al., 2005; Warneck, 2003).
272 They also increased with irradiation time up to 18~24 h in both samples and then gradually
273 decreased (except for MeGly in AA) until the end (120 h) of the experiment (Fig. 4g, i, j).
274 However, the other precursor of C_2 diacid, kC_3 diacid (Kawamura et al., 1996a), showed a
275 decrease with irradiation time throughout the experiment, except for few cases (Fig. 3v)
276 whereas hC_4, a precursor of C_3 diacid (Kawamura et al., 1996a), increased up to 18 h in BA
277 and 24 h in AA and remained relatively high until 72 h and then gradually decreased until the
278 end (120 h) of the experiment (Fig. 3u).

279 In contrast, concentrations of C_4 diacid showed a gradual increase with irradiation time
280 up to 72 h in BA and 96 h in AA followed by a slight decrease in the AA and a sharp
281 decrease in BA (Fig. 3c). Relative abundance of C_4 diacid in total diacids also increased from

8.9% (non-irradiated) to 82% (120 h) in AA and from 6.4% to 88% in BA (Fig. 5). Similarly, C_5 diacid in AA (Fig. 3d) showed a gradual increase with irradiation up to 36 h and stayed almost constant until 96 h followed by a slight decrease. Similar trend was found in BA (Fig. 3d). Both C_6 and C_7 diacids showed an increase with irradiation up to 6~36 h and then a gradual decrease until the end (120 h) of the experiment (Fig. 3e,f). Concentrations of *i*C_4 diacid also increased with irradiation up to 18 h in BA and 36 h in AA and stayed relatively constant until 72 h or 96 h. Then, the concentrations gradually decreased until the end (120 h) of the experiment (Fig. 3l). *i*C_5 and *i*C_6 diacids (Fig. 3m,n) showed very similar trend with their corresponding normal diacids (Fig. 3d,e).

Long-chain (C_8-C_{12}) diacids showed a sharp decrease with irradiation up to 12 h and then a gradual decrease until the end (120 h) of the experiment (Fig. 3g-k). C_8, C_9 and C_{12} diacids became below the detection limit within several hours, particularly in BA. On the other hand, unsaturated aliphatic (M, F, mM, and Ph) and aromatic diacids (*i*-Ph and *t*-Ph) showed a gradual decrease with irradiation, except for few cases during the early stages of the experiment (Fig. 3o-t). Concentrations of kC_7 increased with irradiation time up to 18 h and then decreased gradually until 120 h (Fig. 3w) whereas oxoacids: ωC_3, ωC_7 and ωC_9 acids, showed a gradual decrease with irradiation, except for few cases (Fig. 4b,d,f). On the other hand, ωC_4 acid showed a sharp increase up to 12 h and then a sharp decrease toward 24 h (Fig. 4c). Interestingly, temporal pattern of ωC_8 acid (Fig. 4e) was similar to that of C_4 diacid (Fig. 3c).

Thus the changes in the concentrations of individual diacids, oxoacids and α-dicarbonyls as well as relative abundances of individual diacids in total diacids and mass ratios of selected species in AA and BA found to be similar (Figs. 3-6), although significant differences are recognized between AA and BA samples during irradiation. Such similarities in the temporal variations of diacids and related polar compounds infer that their

307 photochemical formation and degradation pathways in aqueous aerosols (Fig. 7) are almost
308 same between anthropogenic and biogenic aerosols. However, there were significant
309 differences in the rate of formation and/or degradation of diacids and related compounds
310 between AA and BA, which might have been driven by the differences in the abundances of
311 the diacids and related compounds as well as their precursor compounds in the original
312 (non-irradiated) AA and BA samples. In fact, total diacids, oxoacids and α-dicarbonyls were
313 higher in non-irradiated AA than in BA. On the contrary, OC that contains several precursor
314 compounds (including fatty acids) of diacids and related polar compounds is higher in BA
315 than in AA (Table 1).
316
317 **3.4 Production and decomposition of short-chain diacids and related compounds**
318 A sharp increase was observed in the concentrations of ωC_2, ωC_4, Pyr, Gly and MeGly, but
319 not ωC_3, with irradiation up to 18~24 h following a gradual decrease (Fig. 4), demonstrating
320 an enhanced photochemical production of short-chain ($\leq C_4$) oxoacids and α-dicarbonyls
321 during an early stage of photochemical processing. It is likely because ωC_2, Pyr, Gly and
322 MeGly are significantly produced by photochemical oxidation of aliphatic olefins and
323 aromatic hydrocarbons whereas ωC_4 from cyclic olefins and unsaturated fatty acids (Bandow
324 et al., 1985; Hatakeyama et al., 1987; Kawamura et al., 1996a; Lim et al., 2005; Warneck,
325 2003) but ωC_3 may not be significantly produced from any of these precursor compounds
326 (Fig. 7). On the other hand, the increasing trends of mass ratios of C_2 to its precursor
327 compounds: ωC_2, Pyr, Gly and MeGly as well as C_3 (but not C_4) diacid (Carlton et al., 2007;
328 Ervens et al., 2004b; Kawamura et al., 1996a; Lim et al., 2005; Warneck, 2003), were found
329 for BA toward to 120 h (Fig. 6a-e and f). It is noteworthy that $C_3/\omega C_7$ ratios also showed a
330 slight increase, although they are not clear in the later stages of experiment (Fig. 6g),
331 suggesting a potential formation of C_3 diacid via ωC_7 that is derived from unsaturated fatty

332 acids and/or cyclic olefins. In addition, F/M ratios showed an increase with irradiation up to
333 48 h in AA and 18 h in BA followed by a gradual decrease until the end of experiment (Fig.
334 6i), indicating a significant photochemical transformation during an early stage of experiment
335 and decomposition in a later stage.

336 Photochemical degradation of C_2 and C_3 diacids should have overwhelmed their
337 photochemical production even in an early stage of experiment, except for few cases (Fig.
338 3a,b). Diacids and other compounds containing a carbonyl group can form stable carboxylate
339 salts with amines upon photochemical oxidation. However, based on laboratory studies, C_2
340 and C_3 diacids have been reported to decompose in aqueous phase in the presence of Fe^{3+}
341 (and C_2 diacid even in the presence of Fe^{2+}) under UV irradiation at 254 nm as well as at a
342 solar spectrum (>300 nm) (Pavuluri and Kawamura, 2012; Wang et al., 2010b; Zuo and
343 Hoigne, 1994), but C_2 diacid (and maybe C_3 diacid) is relatively stable in the absence of Fe
344 species (Pavuluri and Kawamura, 2012). It is well documented that both C_2 and C_3 diacids
345 have the strongest chelating capacity with Fe^{3+} among all diacids and tend to form mono, di
346 and tri oxalato (equilibrium constant $\log_{10}(b) = 9.4$, 16.2 and 20.4, respectively) and malonato
347 (equilibrium constant $\log_{10}(b) = 7.5$, 13.3 and 16.9, respectively) complexes by acting as
348 ligands in aqueous phase, which exhibit a strong light absorbing ability (Wang et al., 2010b).
349 Although the equilibrium constant of Fe^{3+}-malanato complex is slightly lower than that of
350 Fe^{3+}-oxalato, both diacids photolyze upon the absorption of UV light to result in Fe^{2+} and
351 CO_2 (Wang et al., 2010b; Zuo and Hoigne, 1994).

352 We found that non-irradiated AA and BA samples contain significant amounts of
353 water-soluble Fe^{2+} and Fe^{3+} species (Table 1). Because high abundance of particulate Fe is
354 present in both AA and BA (Table 1), the concentrations of water-soluble Fe^{2+} and Fe^{3+}
355 species in both AA and BA samples may increase upon UV irradiation; the water-insoluble
356 Fe can be transformed into water-soluble forms by photochemical processing of mineral

357 aerosols (Solmon et al., 2009; Srinivas et al., 2012). However, we did not measure the
358 concentrations of Fe^{2+} and Fe^{3+} species in the irradiated samples. In fact, the mass ratio of C_2
359 diacid to Fe^{3+} is 15:1 in non-irradiated AA and 7:1 in BA, which are close to the ratio (10:1)
360 used in laboratory experiments conducted by Pavuluri and Kawamura (2012) for
361 Fe-catalyzed photolysis of C_2 diacid in aqueous phase, in which the photolysis of C_2 is very
362 fast ($k = 206$ L mol^{-1} s^{-1}) and 99% of the C_2 is degraded in 0.5 h. Therefore, available
363 water-soluble Fe^{3+} (and Fe^{2+}) in AA and BA should be enough to promote the catalytic
364 photochemical degradation of C_2 (and C_3) upon UV irradiation (Fig. 7) and thus the
365 degradation rate of C_2 (and C_3) should have increased with the prolonged experiment due to
366 enhancement in Fe^{3+} (and Fe^{2+}) levels in the given sample.

367 The concentration of C_2 diacid in AA decreased by 30% in 1.5 h and continued to
368 decline by 90% until 12 h (Fig. 3a). On the other hand, the experiment of BA showed that the
369 concentration of C_2 decreased by 47% and 51% in 0.5 h and 1.5 h, respectively, and then
370 gradually declined. The concentrations of C_3 also showed similar trends with C_2 (Fig. 3b).
371 Although C_2 and C_3 diacids decreased sharply during early stages of experiment, they
372 decreased gradually in the later stages, despite possibly enhanced levels of water-soluble Fe^{2+}
373 and Fe^{3+} species. These trends imply that photolysis of C_2 and C_3 diacids is highly significant
374 in the presence of water-soluble Fe^{3+} (and Fe^{2+}) (Fig. 7). On the other hand, the formation of
375 both C_2 and C_3 diacids is also intensive with the photochemical processing of their precursor
376 compounds in AA and BA. However, the net rate of production or degradation of C_2 and C_3
377 diacids in each experiment (Figs. 3a,b) should depend on the abundances of water-soluble
378 Fe^{2+} and Fe^{3+} species and their precursors in AA and BA.

379 We found an increase in the mass ratios of MeGly to Gly with irradiation toward the
380 end of the experiment, except for an early stage of experiment (up to 6 h) in AA, whereas in
381 BA they remained relatively constant up to 36 h and then increased gradually up to 72 h

followed by a rapid decrease (Fig. 6n). As noted earlier, concentrations of Gly and MeGly increased with experiment up to 18~24 h in both AA and BA. Thereafter, Gly decreased toward the end of experiment in both AA and BA whereas MeGly remained relatively constant in the AA, but decreased in BA (Fig. 4i,j). Such differences should be caused by the difference in their production rates depending on the concentrations of potential precursors and their oxidation products in AA and BA: benzene and glycolaldehyde for Gly, acetone and higher alkanes ($>C_3$) and alkenes ($>C_2$) for MeGly (Fu et al., 2008), rather than the reaction rates of the Gly (1.1×10^9 M^{-1} S^{-1}) and MeGly (6.44×10^8 M^{-1} S^{-1}) with $HO^{\bullet}$ in aqueous phase (Tan et al., 2012). Therefore, the high abundance of MeGly in AA than Gly can be attributed to its enhanced production than the later species during photochemical processing of aqueous aerosols derived from anthropogenic sources. Further, the oligomerization of Gly and MeGly (Lim et al., 2010; Tan et al., 2009; Tan et al., 2012) might have also played an important role on the changes in their concentrations with irradiation time, however, we did not focus on the measurements of oligomers here because of the analytical limitations.

3.5 Possible photochemical pathways of long-chain diacids and oxoacids

Enhanced concentrations of normal and branched C_4-C_7 diacids during an early stage (18~36 h) (Fig. 3c-f), despite degradation of C_2 and C_3 and longer-chain ($>C_7$) diacids (Fig. 3a, b, g-k), may be caused by photochemical oxidation of the first generation products derived from the oxidation of anthropogenic and/or biogenic VOCs (e.g., cycloalkenes, monoterpenes, and sesquiterpenes) and unsaturated fatty acids (Gao et al., 2004; Kalberer et al., 2000) (Fig. 7). In addition, the photochemical oxidation of the polymers of polyunsaturated fatty acids, if available, can significantly produce the long-chain ($\geq C_4$) diacids (Harvey et al., 1983), a subject of future research. In fact, polyunsaturated fatty acids (e.g., linolenic acid ($C_{18:3}$)) can undergo free radical oxidative cross-linking in the air and produce high molecular weight

407 organic compounds (e.g., fulvic acid) (Harvey et al., 1983; Wheeler, 1972). Harvey et al.
408 (1983) found a series of C_4-C_9 diacids by oxidizing the marine fulvic acid in a laboratory
409 study. On the other hand, the chelating capability of succinate (equilibrium constant $\log_{10}(b)$
410 = 7.5 (Wang et al., 2010b)) and other long-chain diacids with Fe^{3+} is weak and hence, their
411 photolysis is insignificant. However, they should be further oxidized to result in lower diacids
412 (Kawamura et al., 1996a; Matsunaga et al., 1999). The degradation of these diacids should be
413 increased with increasing chain length because the oxidation rate of C_4 to C_9 diacids is
414 increased with increasing carbon number (Yang et al., 2008b).

415 The relatively constant levels of C_5, *i*C_4 and *i*C_5 during 36 h and 72~96 h (Fig. 3d,l,m)
416 may be due to the balance between photochemical production and degradation. The increases
417 in the concentrations of C_4 with a prolonged irradiation up to 72 h in BA and 96 h in AA
418 further demonstrate its formation from higher diacids and other precursors in aqueous
419 aerosols (Charbouillot et al., 2012; Kawamura and Sakaguchi, 1999) (Fig. 7). In fact, total
420 diacids stayed relatively constant from 24 h to 72~96 h (Fig. 3x). In addition, mass ratios of
421 C_4 to C_5-C_7 showed a gradual increase throughout the experiment (until 120 h) in both AA
422 and BA (Fig. 6k-m). These results support a photochemical breakdown of longer-chain ($\geq C_5$)
423 diacids resulting in C_4 (Charbouillot et al., 2012; Matsunaga et al., 1999; Yang et al., 2008b).
424 Yang et al. (2008b) reported that the production of C_4 diacid is predominant followed by C_5
425 diacid during a laboratory photochemical oxidation of C_6-C_9 diacids.

426 In addition, ωC_8 acid, which can be produced by the oxidation of cyclic olefins and
427 unsaturated fatty acids (Gao et al., 2004; Kawamura and Sakaguchi, 1999), showed a gradual
428 increase (Fig. 4e) similar to that of C_4 diacid (Fig. 3c) in both AA and BA, suggesting a
429 significant photochemical production of C_4 via ωC_8 until the consumption of the precursor
430 compounds derived from anthropogenic and biogenic VOCs and biogenic unsaturated fatty
431 acids (Gao et al., 2004; Kalberer et al., 2000). In fact, ratios of C_4 to C_5-C_7 were 10 times

higher in BA than in AA whereas those of C_4/ωC_8 were similar in both the BA and AA (Fig. 6j). However, their temporal profiles with irradiation time are similar in both AA and BA. These results suggest that the formation of C_4 and ωC_8 is much higher in biogenic aerosols than in anthropogenic aerosols compared to C_5-C_7 diacids, but their formation/degradation processes may be similar irrespective of the origin of precursors. However, it is not clear from this study if C_4 is mainly derived (via ωC_8) from cyclic olefins or unsaturated fatty acids (Fig. 7).

It is well established that long-chain (C_8-C_{12}) diacids are formed by photochemical oxidation of unsaturated fatty acids (e.g., oleic acid) (Kawamura and Gagosian, 1987; Matsunaga et al., 1999) (Fig. 7). However, unsaturated fatty acids were not abundant (e.g., oleic acid was 0.89 ng m^{-3} in AA and below detection limit in BA) in non-irradiated samples (Fu et al., 2010). Hence, photochemical formation of long-chain diacids from the oxidation of unsaturated fatty acids should be less important during the experiment, although chemical forms of polymerized and/or partially oxidized unsaturated fatty acids may be abundant in the aerosols. On the other hand, photooxidation rate constant of diacids increases with an increase in carbon number of individual diacids ($\geq C_4$) (Yang et al., 2008b). Hence, photochemical breakdown of C_8-C_{12} diacids to lower diacids (Matsunaga et al., 1999; Yang et al., 2008b) should be very likely (Fig. 7). The gradual decreases of aliphatic unsaturated diacids, aromatic diacids, and oxoacids, except for ωC_8, with irradiation are likely caused by the photochemical degradation (Fig. 7).

3.6 Atmospheric implications

As discussed above, this study reveals that photochemical degradation of C_2 and C_3 (due to Fe-catalyzed photolysis) in aqueous aerosols overwhelmed their production whereas C_4 diacid showed photochemical formation. These results are consistent with the recent

457 atmospheric observations: a significant reduction in C_2 diacid concentration and an inverse
458 relationship between the C_2 and Fe in cloud water (Sorooshian et al., 2013), and the
459 replacement of the predominance of C_2 by C_4 in the Arctic aerosols (Kawamura et al., 2010;
460 Kawamura et al., 2012). It was also reported that C_4 and C_5 diacids are most abundant among
461 C_3-C_8 diacids determined during the photochemical oxidation of C_6-C_9 diacids in a laboratory
462 experiment (Yang et al., 2008b).

463 On the contrary, enhanced degradation of C_2 and C_3 and formation of C_4 diacid upon
464 prolonged irradiation, are not consistent with previous laboratory, observation and model
465 studies on photochemical production and degradation of diacids and related compounds in
466 aqueous phase (e.g., cloud processing) (Carlton et al., 2007; Charbouillot et al., 2012; Ervens
467 et al., 2004b; Kawamura et al., 1996a; Kawamura and Sakaguchi, 1999; Lim et al., 2005;
468 Warneck, 2003). In fact, previous studies did not consider Fe-catalyzed photolysis of C_2
469 diacid, which is significant at least in Fe-rich atmospheric waters. On the other hand, the
470 formation processes and potential precursor compounds of C_4 diacid have not been fully
471 explored yet. Moreover, previous laboratory experiments on aqueous solutions of specific
472 species did not consider the mixing state of organic and inorganic constituents in atmospheric
473 aerosols (Ervens et al., 2011), although simplified experiments sometimes provide useful
474 information on mechanisms.

475 Generally, it has been considered that the anthropogenic contributions of α-dicarbonyls
476 to organic aerosols are minor: 8% for Gly and 5% for MeGly (Fu et al., 2008). To the best of
477 our knowledge, their production in atmospheric waters has not well been recognized yet. Our
478 laboratory experiments indicate that the photochemical production of Gly and MeGly is
479 significant in aqueous aerosols. The production of MeGly is more pronounced compared to
480 Gly with prolonged photochemical processing of aqueous anthropogenic aerosols. Finally,
481 our findings based on the batch laboratory experiment emphasize the importance of the

photolysis of C_2 and C_3 diacids and photochemical production of C_4 diacid and α-dicarbonyls in aqueous aerosols to reconcile the current atmospheric model(s) such as cloud parcel model (Ervens et al., 2004a), and to better understand the secondary organic aerosol budget and its climatic impacts.

4 Summary and conclusions

In this study, we conducted batch UV irradiation experiments on anthropogenic (AA) and biogenic (BA) aerosol samples collected from Chennai, India in the presence of moisture for the reaction time of 0.5 h to 120 h. The irradiated samples were analyzed for molecular compositions of diacids, oxoacids and α-dicarbonyls. Concentrations of C_2 and C_3 and C_8-C_{12} diacids decreased with an increase in 12-24 h. In contrast, C_4 diacid (and C_5-C_7) showed a significant increase with reaction time up to 72 h in BA and 96 h in AA. Oxoacids and α-dicarbonyls showed a significant increase during an early stage of irradiation followed by a gradual decrease in the prolonged experiment, except for ωC_8 acid that showed a pattern similar to C_4 diacid and for methylglyoxal that remained relatively abundant from 24 h to the end of the experiment in AA. The mass ratios of C_2 diacid to its precursors: glyoxylic acid, pyruvic acid, α-dicarbonyls (glyoxyal and methylglyoxal) and C_3, showed a considerable increase with irradiation, while those of C_4 to C_5-C_7 diacids and ωC_8 acid and methylglyoxal to glyoxal in AA showed a significant increase with irradiation. These results demonstrate that degradation of C_2 and C_3 (and C_8-C_{12}) and formation of C_4 (and C_5-C_7) is enhanced with photochemical processing of aqueous aerosols. This study further infers that iron-catalyzed photolysis of C_2 and C_3 diacids and photochemical formation of C_4 diacid via ωC_8 acid derived from cyclic olefins and/or unsaturated fatty acids play an important role in controlling their abundances in the atmosphere with photochemical processing of aqueous

aerosols. This study also suggests that photochemical production of α-dicarbonyls, in particular methylglyoxal, in anthropogenic aerosols is significant.

Acknowledgements. This study was in part supported by Japan Society for the Promotion of Science (JSPS) (Grant-in-aid Nos.19204055 and 24221001). C. M. Pavuluri appreciates the financial support from JSPS Fellowship and thanks to two anonymous reviewers.

References

Albrecht, B. A.: Aerosols, cloud microphysics, and fractional cloudiness, Science, 245, 1227-1230, 1989.

Arakaki, T. and Faust, B. C.: Sources, sinks, and mechanisms of hydroxyl radical (•OH) photoproduction and consumption in authentic acidic continental cloud waters from Whiteface Mountain, New York: The role of the Fe(r) (r=II, III) photochemical cycle, J Geophys Res-Atmos, 103, 3487-3504, 1998.

Bandow, H., Washida, N. and Akimoto, H.: Ring-Cleavage Reactions of Aromatic-Hydrocarbons Studied by Ft-Ir Spectroscopy .1. Photooxidation of Toluene and Benzene in the Nox-Air System, B Chem Soc Jpn, 58, 2531-2540, 1985.

Carlton, A. G., Turpin, B. J., Lim, H. J., Altieri, K. E. and Seitzinger, S.: Link between isoprene and secondary organic aerosol (SOA): Pyruvic acid oxidation yields low volatility organic acids in clouds, Geophys Res Lett, 33, L06822, L06822, doi: 10.1029/2005gl025374, 2006.

Carlton, A. G., Turpin, B. J., Altieri, K. E., Seitzinger, S., Reff, A., Lim, H. J. and Ervens, B.: Atmospheric oxalic acid and SOA production from glyoxal: Results of aqueous photooxidation experiments, Atmos Environ, 41, 7588-7602, 2007.

Carter, W. P. L. and Atkinson, R.: Development and evaluation of a detailed mechanism for the atmospheric reactions of isoprene and NOx, Int J Chem Kinet, 28, 497-530, 1996.

Charbouillot, T., Gorini, S., Voyard, G., Parazols, M., Brigante, M., Deguillaume, L., Delort, A. M. and Mailhot, G.: Mechanism of carboxylic acid photooxidation in atmospheric aqueous phase: Formation, fate and reactivity, Atmos Environ, 56, 1-8, doi:10.1016/J.Atmosenv.2012.03.079, 2012.

Chebbi, A. and Carlier, P.: Carboxylic acids in the troposphere, occurrence, sources, and sinks: A review, Atmos Environ, 30, 4233-4249, 1996.

Ervens, B., Feingold, G., Clegg, S. L. and Kreidenweis, S. M.: A modeling study of aqueous production of dicarboxylic acids: 2. Implications for cloud microphysics, J Geophys Res-Atmos, 109, D15206, doi:10.1029/2004jd004575, 2004a.

Ervens, B., Feingold, G., Frost, G. J. and Kreidenweis, S. M.: A modeling study of aqueous production of dicarboxylic acids: 1. Chemical pathways and speciated organic mass production, J Geophys Res-Atmos, 109, D15205, doi:10.1029/2003jd004387, 2004b.

544 Ervens, B., Turpin, B. J. and Weber, R. J.: Secondary organic aerosol formation in cloud
545 droplets and aqueous particles (aqSOA): a review of laboratory, field and model studies,
546 Atmos Chem Phys, 11, 11069-11102, doi:10.5194/Acp-11-11069-2011, 2011.
547 Fu, P. Q., Kawamura, K., Pavuluri, C. M., Swaminathan, T. and Chen, J.: Molecular
548 characterization of urban organic aerosol in tropical India: contributions of primary
549 emissions and secondary photooxidation, Atmos Chem Phys, 10, 2663-2689, 2010.
550 Fu, T. M., Jacob, D. J., Wittrock, F., Burrows, J. P., Vrekoussis, M. and Henze, D. K.: Global
551 budgets of atmospheric glyoxal and methylglyoxal, and implications for formation of
552 secondary organic aerosols, J Geophys Res-Atmos, 113, D15303,
553 doi:10.1029/2007JD009505, 2008.
554 Gao, S., Keywood, M., Ng, N. L., Surratt, J., Varutbangkul, V., Bahreini, R., Flagan, R. C.
555 and Seinfeld, J. H.: Low-molecular-weight and oligomeric components in secondary
556 organic aerosol from the ozonolysis of cycloalkenes and α-pinene, J Phys Chem A, 108,
557 10147-10164, 2004.
558 Garg, A., Bhattacharya, S., Shukla, P. R. and Dadhwal, W. K.: Regional and sectoral
559 assessment of greenhouse gas emissions in India, Atmos Environ, 35, 2679-2695, 2001.
560 Giebl, H., Berner, A., Reischl, G., Puxbaum, H., Kasper-Giebl, A. and Hitzenberger, R.:
561 CCN activation of oxalic and malonic acid test aerosols with the University of Vienna
562 cloud condensation nuclei counter, J Aerosol Sci, 33, 1623-1634, 2002.
563 Harvey, G. R., Boran, D. A., Chesal, L. A. and Tokar, J. M.: The Structure of Marine Fulvic
564 and Humic Acids, Mar Chem, 12, 119-132, 1983.
565 Hatakeyama, S., Ohno, M., Weng, J. H., Takagi, H. and Akimoto, H.: Mechanism for the
566 Formation of Gaseous and Particulate Products from Ozone-Cycloalkene Reactions in Air,
567 Environ Sci Technol, 21, 52-57, 1987.
568 Kalberer, M., Yu, J., Cocker, D. R., Flagan, R. C. and Seinfeld, J. H.: Aerosol formation in
569 the cyclohexene-ozone system, Environ Sci Technol, 34, 4894-4901, 2000.
570 Kanakidou, M., Seinfeld, J. H., Pandis, S. N., Barnes, I., Dentener, F. J., Facchini, M. C., Van
571 Dingenen, R., Ervens, B., Nenes, A., Nielsen, C. J., Swietlicki, E., Putaud, J. P.,
572 Balkanski, Y., Fuzzi, S., Horth, J., Moortgat, G. K., Winterhalter, R., Myhre, C. E. L.,
573 Tsigaridis, K., Vignati, E., Stephanou, E. G. and Wilson, J.: Organic aerosol and global
574 climate modelling: a review, Atmos. Chem. Phys., 5, 1053-1123, 2005.

575 Kawamura, K. and Gagosian, R. B.: Implications of ω-oxocarboxylic acids in the remote
576 marine atmosphere for photooxidation of unsaturated fatty acids, Nature, 325, 330-332,
577 1987.
578 Kawamura, K. and Kaplan, I. R.: Motor exhaust emissions as a primary source for
579 dicarboxylic acids in Los-Angeles ambient air, Environ Sci Technol, 21, 105-110, 1987.
580 Kawamura, K.: Identification of C2-C10 ω-oxocarboxylic acids, pyruvic acid, and C2-C3
581 α-dicarbonyls in wet precipitation and aerosol samples by capillary GC and GC/MS,
582 Anal Chem, 65, 3505-3511, 1993.
583 Kawamura, K. and Ikushima, K.: Seasonal changes in the distribution of dicarboxylic acids in
584 the urban atmosphere, Environ Sci Technol, 27, 2227-2235, 1993.
585 Kawamura, K., Kasukabe, H. and Barrie, L. A.: Source and reaction pathways of
586 dicarboxylic acids, ketoacids and dicarbonyls in arctic aerosols: One year of observations,
587 Atmos. Environ., 30, 1709-1722, 1996a.
588 Kawamura, K., Semere, R., Imai, Y., Fujii, Y. and Hayashi, M.: Water soluble dicarboxylic
589 acids and related compounds in Antarctic aerosols, J Geophys Res-Atmos, 101,
590 18721-18728, 1996b.
591 Kawamura, K. and Sakaguchi, F.: Molecular distributions of water soluble dicarboxylic acids
592 in marine aerosols over the Pacific Ocean including tropics, J Geophys Res-Atmos, 104,
593 3501-3509, 1999.
594 Kawamura, K., Yokoyama, K., Fujii, Y. and Watanabe, O.: A Greenland ice core record of
595 low molecular weight dicarboxylic acids, ketocarboxylic acids, and α-dicarbonyls: A
596 trend from Little Ice Age to the present (1540 to 1989 AD), J Geophys Res-Atmos, 106,
597 1331-1345, 2001.
598 Kawamura, K., Kasukabe, H. and Barrie, L. A.: Secondary formation of water-soluble
599 organic acids and α-dicarbonyls and their contributions to total carbon and
600 water-soluble organic carbon: Photochemical aging of organic aerosols in the Arctic
601 spring, J Geophys Res-Atmos, 115, D21306 DOI: 21310.21029/22010JD014299, 2010.
602 Kawamura, K., Ono, K., Tachibana, E., Charriere, B. and Sempere, R.: Distributions of low
603 molecular weight dicarboxylic acids, ketoacids and α-dicarbonyls in the marine aerosols
604 collected over the Arctic Ocean during late summer, Biogeosciences, 9, 4725-4737, 2012.
605 Lelieveld, J., Crutzen, P. J., Ramanathan, V., Andreae, M. O., Brenninkmeijer, C. A. M.,
606 Campos, T., Cass, G. R., Dickerson, R. R., Fischer, H., de Gouw, J. A., Hansel, A.,
607 Jefferson, A., Kley, D., de Laat, A. T. J., Lal, S., Lawrence, M. G., Lobert, J. M.,

608 Mayol-Bracero, O. L., Mitra, A. P., Novakov, T., Oltmans, S. J., Prather, K. A., Reiner,
609 T., Rodhe, H., Scheeren, H. A., Sikka, D. and Williams, J.: The Indian ocean experiment:
610 widespread air pollution from South and Southeast Asia, Science, 291, 1031-1036, 2001.
611 Lim, H. J., Carlton, A. G. and Turpin, B. J.: Isoprene forms secondary organic aerosol
612 through cloud processing: model simulations, Environ Sci Technol, 39, 4441-4446, Doi
613 10.1021/Es048039h, 2005.
614 Lim, Y. B., Tan, Y., Perri, M. J., Seitzinger, S. P. and Turpin, B. J.: Aqueous chemistry and
615 its role in secondary organic aerosol (SOA) formation, Atmos Chem Phys, 10,
616 10521-10539, Doi 10.5194/Acp-10-10521-2010, 2010.
617 Mahowald, N., Jickells, T. D., Baker, A. R., Artaxo, P., Benitez-Nelson, C. R., Bergametti,
618 G., Bond, T. C., Chen, Y., Cohen, D. D., Herut, B., Kubilay, N., Losno, R., Luo, C.,
619 Maenhaut, W., McGee, K. A., Okin, G. S., Siefert, R. L. and Tsukuda, S.: Global
620 distribution of atmospheric phosphorus sources, concentrations, and deposition rates, and
621 anthropogenic impacts, Global Biogeochem Cy, 22, GB4026,
622 doi:10.1029/2008GB003240, 2008.
623 Matsunaga, S., Kawamura, K., Nakatsuka, T. and Ohkouchi, N.: Preliminary study on
624 laboratory photochemical formation of low molecular weight dicarboxylic acids from
625 unsaturated fatty acid (oleic acid), Res. Org. Geochem., 14, 19-25, 1999.
626 Narukawa, M., Kawamura, K., Takeuchi, N. and Nakajima, T.: Distribution of dicarboxylic
627 acids and carbon isotopic compositions in aerosols from 1997 Indonesian forest fires,
628 Geophys. Res. Lett., 26, 3101-3104, 1999.
629 Noziere, B., Ekstrom, S., Alsberg, T. and Holmstrom, S.: Radical-initiated formation of
630 organosulfates and surfactants in atmospheric aerosols, Geophys Res Lett, 37, Artn
631 L05806
632 Doi 10.1029/2009gl041683, 2010.
633 Pacyna, J. M. and Pacyna, E. G.: An assessment of global and regional emissions of trace
634 metals to the atmosphere from anthropogenic sources worldwide, Environmental Reviews,
635 9, 269-298, 2001.
636 Padhy, P. K. and Varshney, C. K.: Emission of volatile organic compounds (VOC) from
637 tropical plant species in India, Chemosphere, 59, 1643-1653, 2005.
638 Pavuluri, C. M., Kawamura, K. and Swaminathan, T.: Water-soluble organic carbon,
639 dicarboxylic acids, ketoacids, and α-dicarbonyls in the tropical Indian aerosols, J
640 Geophys Res-Atmos, 115, D11302, D11302, doi:10.1029/2009jd012661, 2010.

641 Pavuluri, C. M., Kawamura, K., Aggarwal, S. G. and Swaminathan, T.: Characteristics,
642 seasonality and sources of carbonaceous and ionic components in the tropical aerosols
643 from Indian region, Atmos Chem Phys, 11, 8215-8230, doi:10.5194/Acp-11-8215-2011,
644 2011.
645 Pavuluri, C. M. and Kawamura, K.: Evidence for 13-carbon enrichment in oxalic acid via
646 iron catalyzed photolysis in aqueous phase, Geophys Res Lett, 39, L03802, L03802,
647 doi:10.1029/2011gl050398, 2012.
648 Reddy, M. S. and Venkataraman, C.: Inventory of aerosol and sulphur dioxide emissions
649 from India: I - Fossil fuel combustion, Atmos Environ, 36, 677-697, 2002a.
650 Reddy, M. S. and Venkataraman, C.: Inventory of aerosol and sulphur dioxide emissions
651 from India. Part II - biomass combustion, Atmos Environ, 36, 699-712, 2002b.
652 Saxena, P. and Hildemann, L. M.: Water-soluble organics in atmospheric particles: A critical
653 review of the literature and application of thermodynamics to identify candidate
654 compounds, J. Atmos. Chem., 24, 57-109, 1996.
655 Solmon, F., Chuang, P. Y., Meskhidze, N. and Chen, Y.: Acidic processing of mineral dust
656 iron by anthropogenic compounds over the north Pacific Ocean, J Geophys Res-Atmos,
657 114, D02305, doi:10.1029/2008JD010417, 2009.
658 Sorooshian, A., Wang, Z., Coggon, M. M., Jonsson, H. H. and Ervens, B.: Observations of
659 Sharp Oxalate Reductions in Stratocumulus Clouds at Variable Altitudes: Organic Acid
660 and Metal Measurements During the 2011 E-PEACE Campaign, Environ Sci Technol, 47,
661 7747-7756, Doi 10.1021/Es4012383, 2013.
662 Srinivas, B., Sarin, M. M. and Kumar, A.: Impact of anthropogenic sources on aerosol iron
663 solubility over the Bay of Bengal and the Arabian Sea, Biogeochemistry, 110, 257-268,
664 2012.
665 Stookey, L. C.: Ferrozine - a new spectrophotometric reagent for iron, Anal Chem, 42,
666 779-781, 1970.
667 Tan, Y., Perri, M. J., Seitzinger, S. P. and Turpin, B. J.: Effects of Precursor Concentration
668 and Acidic Sulfate in Aqueous Glyoxal-OH Radical Oxidation and Implications for
669 Secondary Organic Aerosol, Environ Sci Technol, 43, 8105-8112, Doi
670 10.1021/Es901742f, 2009.
671 Tan, Y., Lim, Y. B., Altieri, K. E., Seitzinger, S. P. and Turpin, B. J.: Mechanisms leading to
672 oligomers and SOA through aqueous photooxidation: insights from OH radical oxidation
673 of acetic acid and methylglyoxal, Atmos Chem Phys, 12, 801-813, 2012.

674 Theodosi, C., Markaki, Z. and Mihalopoulos, N.: Iron speciation, solubility and temporal
675 variability in wet and dry deposition in the Eastern Mediterranean, Mar Chem, 120,
676 100-107, 2010a.
677 Theodosi, C., Markaki, Z., Tselepides, A. and Mihalopoulos, N.: The significance of
678 atmospheric inputs of soluble and particulate major and trace metals to the eastern
679 Mediterranean seawater, Mar Chem, 120, 154-163, 2010b.
680 Tilgner, A. and Herrmann, H.: Radical-driven carbonyl-to-acid conversion and acid
681 degradation in tropospheric aqueous systems studied by CAPRAM, Atmos Environ, 44,
682 5415-5422, Doi 10.1016/J.Atmosenv.2010.07.050, 2010.
683 Twomey, S.: Influence of pollution on shortwave albedo of clouds, J Atmos Sci, 34,
684 1149-1152, 1977.
685 Wang, G., Xie, M., Hu, S., Gao, S., Tachibana, E. and Kawamura, K.: Dicarboxylic acids,
686 metals and isotopic compositions of C and N in atmospheric aerosols from inland China:
687 implications for dust and coal burning emission and secondary aerosol formation, Atmos
688 Chem Phys, 10, 6087-6096, 10.5194/acp-10-6087-2010, 2010a.
689 Wang, Z. H., Chen, X., Ji, H. W., Ma, W. H., Chen, C. C. and Zhao, J. C.: Photochemical
690 cycling of iron mediated by dicarboxylates: special effect of malonate, Environ Sci
691 Technol, 44, 263-268, Doi 10.1021/Es901956x, 2010b.
692 Warneck, P.: In-cloud chemistry opens pathway to the formation of oxalic acid in the marine
693 atmosphere, Atmos Environ, 37, 2423-2427, Doi 10.1016/S1352-2310(03)00136-5, 2003.
694 Wheeler, J.: Some Effects of Solar Levels of Ultraviolet-Radiation on Lipids in Artificial
695 Sea-Water, J Geophys Res, 77, 5302-&, 1972.
696 Yang, L. M., Ray, M. B. and Yu, L. E.: Photooxidation of dicarboxylic acids- Part 1: effects
697 of inorganic ions on degradation of azelaic acid, Atmos Environ, 42, 856-867, 2008a.
698 Yang, L. M., Ray, M. B. and Yu, L. E.: Photooxidation of dicarboxylic acids- Part II:
699 Kinetics, intermediates and field observations, Atmos Environ, 42, 868-880, Doi
700 10.1016/J.Atmosenv.2007.10.030, 2008b.
701 Zuo, Y. G. and Hoigne, J.: Photochemical decomposition of oxalic, glyoxalic and pyruvic
702 acid catalyzed by iron in atmospheric waters, Atmos Environ, 28, 1231-1239, 1994.
703
704

705 **Table 1.** Concentrations of carbonaceous components, organic molecular tracer compounds,
706 diacids and related compounds, trace elements, metals and water-soluble iron species in
707 non-irradiated IND104 (anthropogenic aerosols: AA) and IND178 (biogenic aerosols: BA)
708 aerosol samples collected from Chennai, India.

	Concentrations (ng m^{-3})	
	IND104 (AA)	IND178 (BA)
Organic carbon[a]	6400	9820
Elemental carbon[a]	4810	1810
Levoglucosan[b]	79.1	158
Hopanes (C_{27}-C_{35}) [b]	11.8	3.9
Fatty acids (C_8-C_{34}) [b]	167	297
Fatty alcohols (C_{14}-C_{34}) [b]	93.3	178
Total diacids	1030	640
Total oxoaxids	110	62.2
Total α-dicarbonyls	10.9	11.6
Al	15100	914
Ca	1640	0.00
Cd	10.7	1.73
Co	1.07	0.00
Cr	5.33	0.00
Cu	796	13.9
Fe	2070	553
K	1220	893
Mg	679	90.2
Mn	129	19.1
Na	1890	408
Ni	58.7	106
P	62.9	0.00
Pb	133	39.9
S	4640	5820
Sb	13.9	29.5
V	9.60	0.00
Zn	2030	137
Fe_{WS}[c]	57.0	78.3
Fe^{2+}	20.5	30.0
Fe^{3+}	36.6	48.4

709 [a]: Data is obtained from Pavuluri et al. (2011), [b]: Data is obtained from Fu et al. (2010), [c]:
710 Fe_{WS} is water-soluble Fe.

711 **Figure Captions**

712 **Fig. 1.** A map of South Asia with sampling site, Chennai (13.04°N; 80.17°E), India together
713 with plots of 10-day air mass trajectories arriving at 500 m a.g.l. over Chennai, India.

714 **Fig. 2.** Schematic of experimental setup for irradiation of atmospheric aerosol filter sample.

715 **Fig. 3.** Changes in concentrations of individual dicarboxylic acids and total diacids as a
716 function of UV irradiation time in anthropogenic (AA) and biogenic aerosols (BA).

717 **Fig. 4.** Changes in concentrations of individual oxoacids and α-dicarbonyls and total
718 oxoacids and α-dicarbonyls as a function of UV irradiation time in AA and BA.

719 **Fig. 5.** Changes in relative abundances of straight chain diacids (C_2-C_{10}) to total diacids as a
720 function of UV irradiation time in AA and BA.

721 **Fig. 6.** Changes in mass ratios of selected diacids, oxoacids and α-dicarbonyls as a function
722 of UV irradiation time in AA and BA.

723 **Fig. 7.** Possible photochemical formation and/or degradation pathways of diacids, oxoacids
724 and α-dicarbonyls in aqueous aerosols.

725 **Fig. 1.**

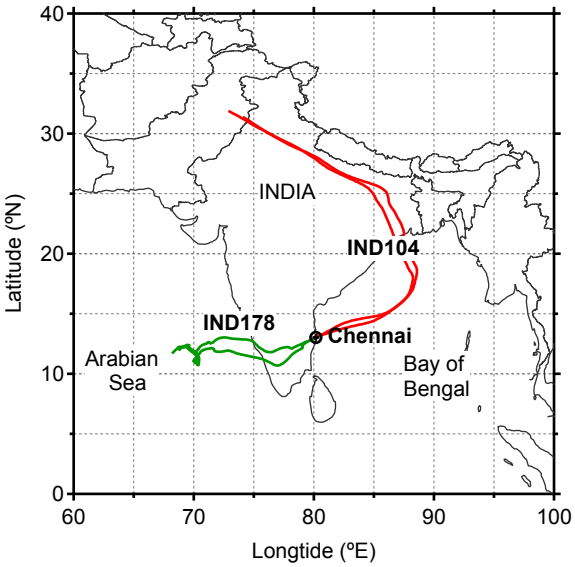
40
30
20
10
0
60
70
80
90
100
Latitude (ºN)
Longtide (ºE)
INDIA
IND104
IND178
Chennai
Arabian
Sea
Bay of
Bengal

726

727 **Fig. 2.**

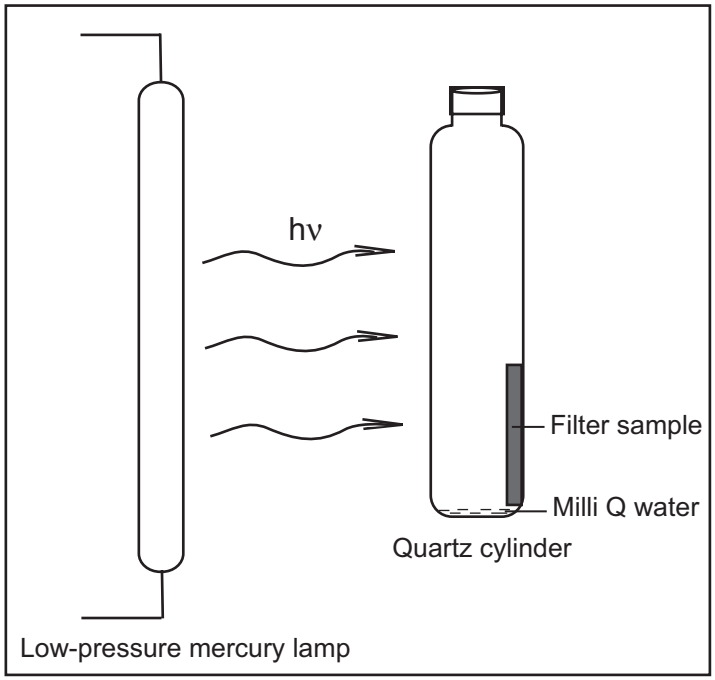
hν
Filter sample
Milli Q water
Quartz cylinder
Low-pressure mercury lamp

728

729 **Fig. 3.**

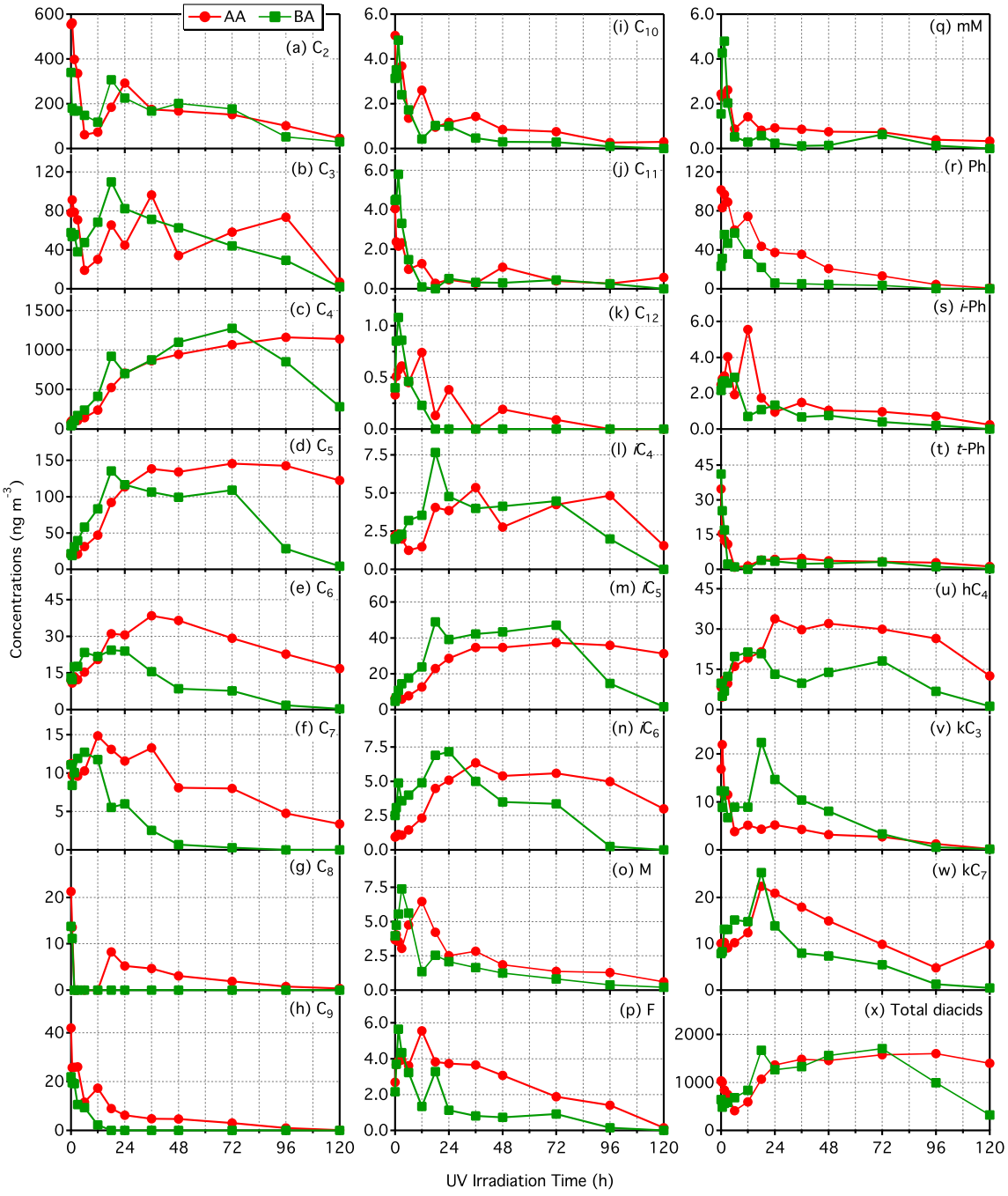
AA
BA
(a) C2
(b) C3
(c) C4
(d) C5
(e) C6
(f) C7
(g) C8
(h) C9
(i) C10
(j) C11
(k) C12
(l) iC4
(m) iC5
(n) iC6
(o) M
(p) F
(q) mM
(r) Ph
(s) i-Ph
(t) t-Ph
(u) hC4
(v) kC3
(w) kC7
(x) Total diacids
Concentrations (ng m-3)
UV Irradiation Time (h)

730

731 **Fig. 4.**

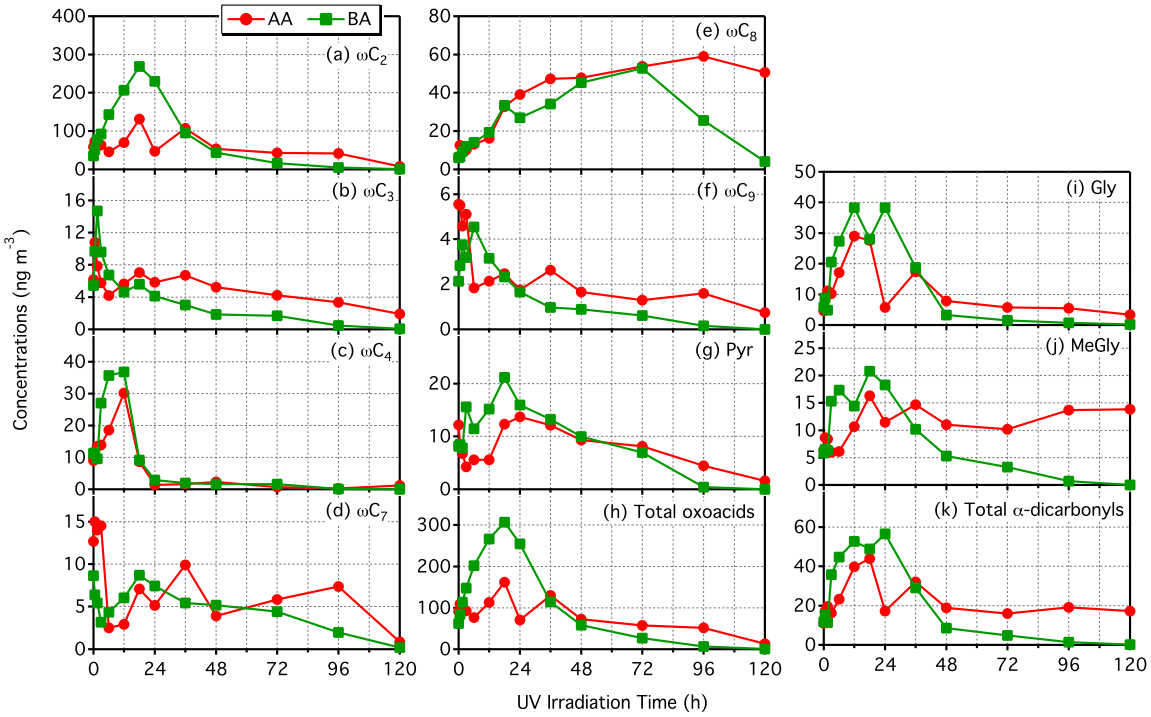
AA
BA
(a) ωC2
(b) ωC3
(c) ωC4
(d) ωC7
(e) ωC8
(f) ωC9
(g) Pyr
(h) Total oxoacids
(i) Gly
(j) MeGly
(k) Total α-dicarbonyls
Concentrations (ng m-3)
UV Irradiation Time (h)

732

733 **Fig. 5.**

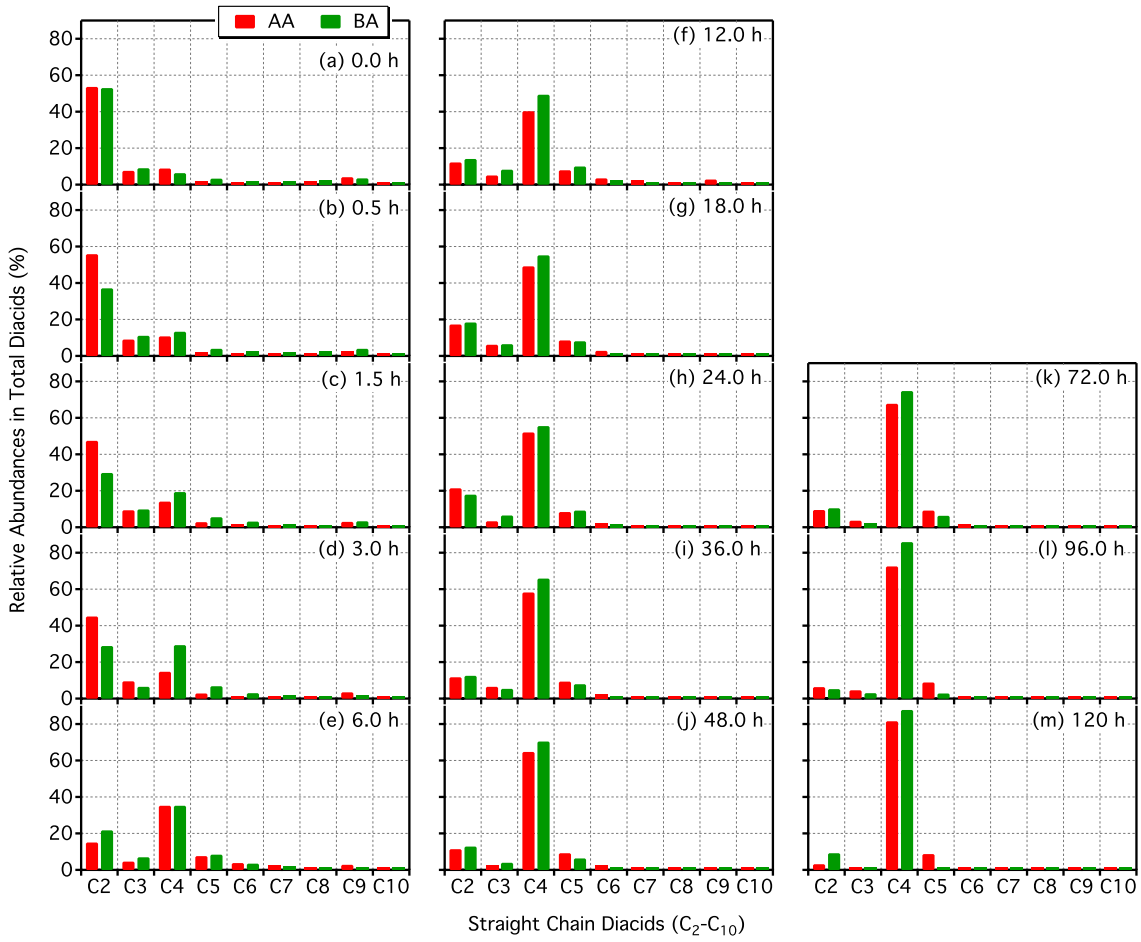
AA
BA
(a) 0.0 h
(b) 0.5 h
(c) 1.5 h
(d) 3.0 h
(e) 6.0 h
(f) 12.0 h
(g) 18.0 h
(h) 24.0 h
(i) 36.0 h
(j) 48.0 h
(k) 72.0 h
(l) 96.0 h
(m) 120 h
Relative Abundances in Total Diacids (%)
0
20
40
60
80
C2 C3 C4 C5 C6 C7 C8 C9 C10
Straight Chain Diacids (C_2-C_{10})

734

735 **Fig. 6.**

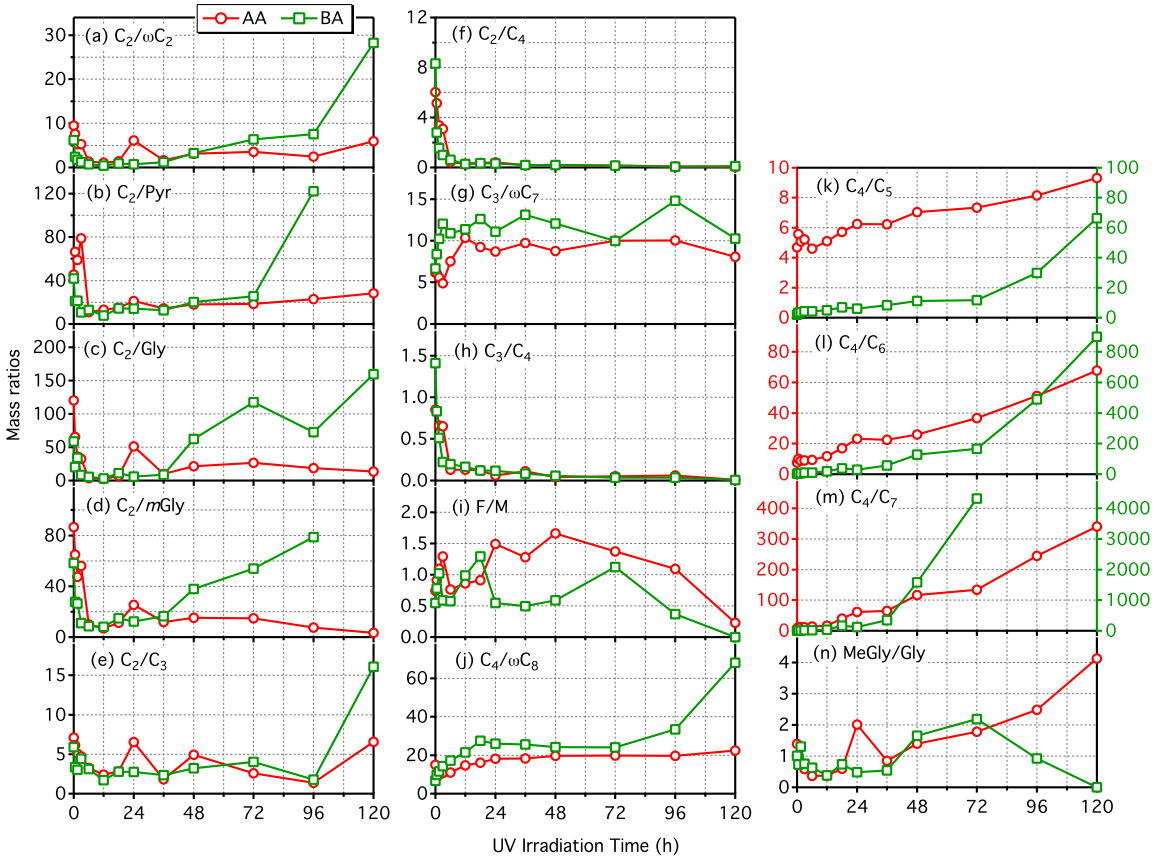
AA
BA
(a) C2/ωC2
(b) C2/Pyr
(c) C2/Gly
(d) C2/mGly
(e) C2/C3
(f) C2/C4
(g) C3/ωC7
(h) C3/C4
(i) F/M
(j) C4/ωC8
(k) C4/C5
(l) C4/C6
(m) C4/C7
(n) MeGly/Gly
Mass ratios
UV Irradiation Time (h)

736

737 **Fig. 7.**

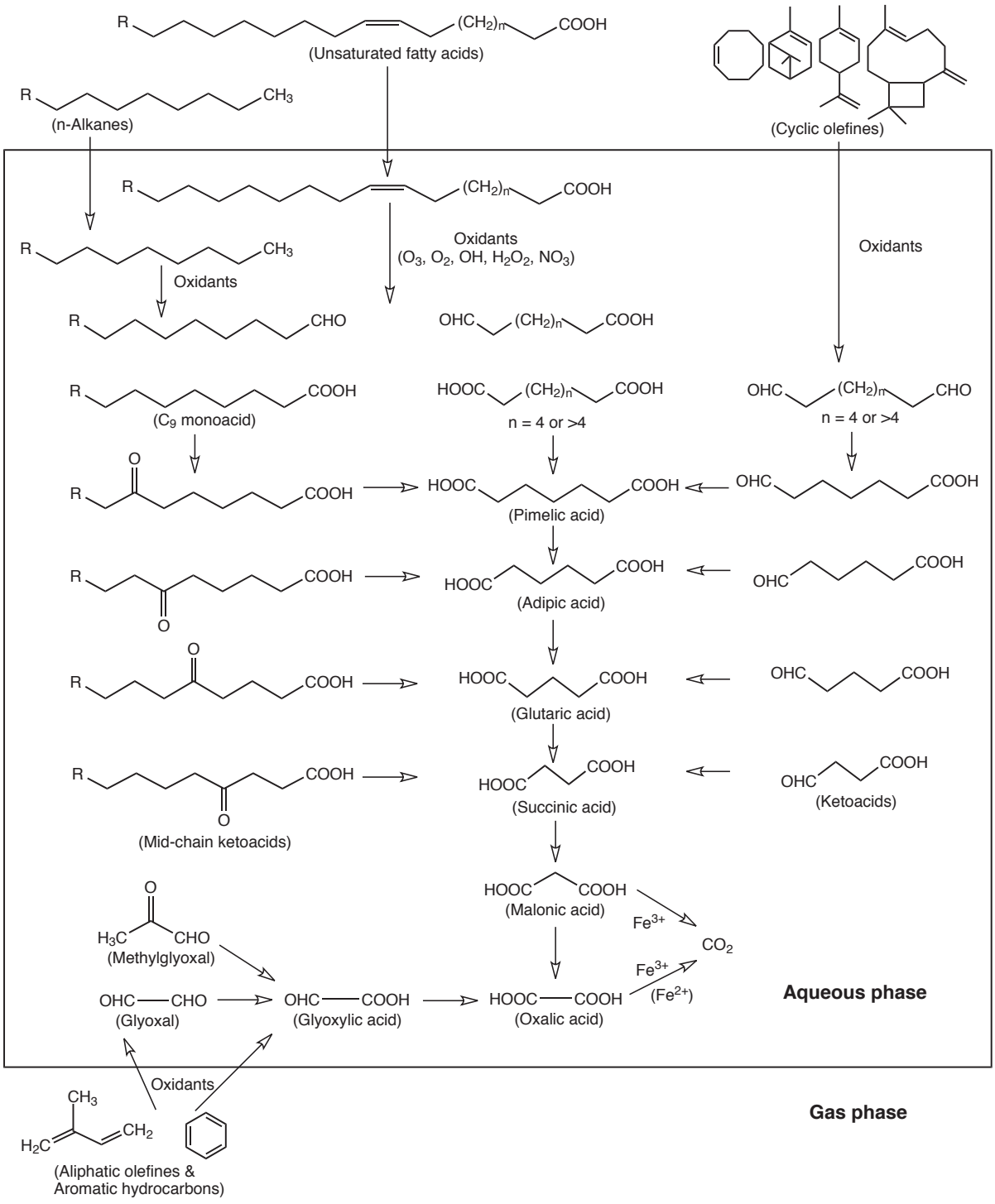
(Unsaturated fatty acids)
(n-Alkanes)
(Cyclic olefines)
Oxidants
(O3, O2, OH, H2O2, NO3)
Oxidants
Oxidants
(C9 monoacid)
n = 4 or >4
n = 4 or >4
(Pimelic acid)
(Adipic acid)
(Glutaric acid)
(Succinic acid)
(Ketoacids)
(Mid-chain ketoacids)
(Malonic acid)
(Methylglyoxal)
(Glyoxal)
(Glyoxylic acid)
(Oxalic acid)
Aqueous phase
Gas phase
Oxidants
(Aliphatic olefines &
Aromatic hydrocarbons)

738